Hongxia Ren,[1] Taylor Y. Lu,[1] Timothy E. McGraw,[2] and Domenico Accili[1]

Anorexia and Impaired Glucose Metabolism in Mice With Hypothalamic Ablation of Glut4 Neurons

Diabetes 2015;64:405–417 | DOI: 10.2337/db14-0752

The central nervous system (CNS) uses glucose independent of insulin. Nonetheless, insulin receptors and insulin-responsive glucose transporters (Glut4) often colocalize in neurons (Glut4 neurons) in anatomically and functionally distinct areas of the CNS. The apparent heterogeneity of Glut4 neurons has thus far thwarted attempts to understand their function. To answer this question, we used Cre-dependent, diphtheria toxin–mediated cell ablation to selectively remove basal hypothalamic Glut4 neurons and investigate the resulting phenotypes. After Glut4 neuron ablation, mice demonstrate altered hormone and nutrient signaling in the CNS. Accordingly, they exhibit negative energy balance phenotype characterized by reduced food intake and increased energy expenditure, without locomotor deficits or gross neuronal abnormalities. Glut4 neuron ablation affects orexigenic melanin-concentrating hormone neurons but has limited effect on neuropeptide Y/agouti-related protein and proopiomelanocortin neurons. The food intake phenotype can be partially normalized by GABA administration, suggesting that it arises from defective GABAergic transmission. Glut4 neuron–ablated mice show peripheral metabolic defects, including fasting hyperglycemia and glucose intolerance, decreased insulin levels, and elevated hepatic gluconeogenic genes. We conclude that Glut4 neurons integrate hormonal and nutritional cues and mediate CNS actions of insulin on energy balance and peripheral metabolism.

The central nervous system (CNS) plays an integral role in maintaining glucose homeostasis (1). It exerts systemic effects on organismal turnover and storage of glucose by promoting hormone release and through sympathetic and parasympathetic innervation of peripheral organs (2). In addition, the CNS is a target organ of diabetes complications, such as stroke, hypoglycemia unawareness, as well as sympathetic dysfunction, not to mention the long-standing and poorly understood relationship between cognitive dysfunction and diabetes (3). Despite the established role of the CNS in metabolism, the identities of effector neurons remain elusive.

We have previously shown that the insulin-responsive glucose transporter, Glut4, is a marker of a distinct subset of neurons (4). We are agnostic as to the function of Glut4 itself in these neurons, but we have pursued the hypothesis that it represents a vestigial marker of their regulatory metabolic functions. This concept is borne out by the finding that ablating insulin receptors (InsR) in a constellation of Glut4-expressing tissues (muscle, fat, and neurons) causes overt diabetes (4), in contrast with the mild metabolic phenotypes observed following InsR knockout in either muscle, fat, or both (5). These findings highlight the potential metabolic function of InsR signaling in Glut4 neurons, as well as the latter's distinct neuroanatomical identity.

Previous studies identified Glut4 expression in the brain (6,7). We have found Glut4-expressing neurons in the CNS among cortical pyramidal neurons, cerebellar Purkinje-like, olfactory bulb, hippocampal, and hypothalamic neurons (4). Given their anatomic and morphological differences, Glut4 neurons are likely to mediate

[1]Department of Medicine and Naomi Berrie Diabetes Center, Columbia University College of Physicians and Surgeons, New York, NY
[2]Department of Biochemistry, Weill Cornell Medical College, New York, NY
Corresponding author: Domenico Accili, da230@cumc.columbia.edu.

Received 12 May 2014 and accepted 20 August 2014.

This article contains Supplementary Data online at http://diabetes.diabetesjournals.org/lookup/suppl/doi:10.2337/db14-0752/-/DC1.

several processes. To begin to clarify their metabolic contribution, we combined cell ablation and metabolic profiling studies to interrogate their hypothalamic functions. Ablation of hypothalamic Glut4-expressing neurons resulted in anorexia and fasting hyperglycemia, altering the response to insulin and leptin. We propose that hypothalamic Glut4 neurons constitute a distinct neuronal entity and mediate CNS effects on energy balance and peripheral metabolism.

RESEARCH DESIGN AND METHODS

Mice

Gt(Rosa)26Sor$^{tm9(CAG\text{-}tdTomato)Hze}$ and C57BL/6-*Gt(ROSA)26Sor*$^{tm1(HBEGF)Awai/J}$ mice were from The Jackson Laboratory. The Columbia University Animal Care and Utilization Committee approved all procedures. Normal chow diet (NCD) had 62.1% calories from carbohydrates, 24.6% from protein, and 13.2% from fat (PicoLab rodent diet 20, 5053; Purina Mills); high-fat diet (HFD) had 20% calories from carbohydrates, 20% from protein, and 60% from fat (D12492; Research Diets). We measured weight and length to calculate BMI and estimated body composition by nuclear magnetic resonance (Bruker Optics). We generated *Glut4-Cre;Rosa-iDTR* and *Pomc-Cre;Rosa-iDTR* mice by mating *Glut4-Cre* or *Pomc-Cre* male transgenic mice with female *Rosa-iDTR* mice and genotyped them as previously described (4).

Metabolic Analyses

We measured food intake and refeeding response as described (8) using a TSE Labmaster Platform (TSE Systems) for indirect calorimetry and activity measurements (9). We used ELISA for leptin, insulin, and glucagon measurements (Millipore) and colorimetric assays for metabolite measurement (4).

Stereotactic Injections

We performed stereotactic manipulations in 3- to 4-month-old mice. We placed cannulae and allowed 1 week for recovery (bilateral targeting −1.5 mm anterior and 0.4 mm lateral to bregma and 4.7 mm below the skull surface). We verified correct positioning of the cannulae by injecting methylene blue (1%) after killing. To ablate cells, we injected diphtheria toxin A (DTA) at a dose of 4 ng/mouse (injector with 1-mm projection). Control mice (carrying *Rosa-DTR* allele) are littermates of Glut4 neuron–ablated mice (carrying *Glut4-Cre;Rosa-DTR* alleles). Both control and Glut4 neuron–ablated mice received DTA injection. Only mice carrying *Glut4-Cre;Rosa-DTR* alleles are susceptible to DTA-mediated cell death. To trace neuronal projection, we injected Ad-iZ-EGfpf 1 μL to the bilateral cannula. For GABA infusion, Alzet 14-day micro-osmotic pumps (model 1002; Durect, Cupertino, CA) loaded with bretazenil (60 ng/mL in saline plus 0.2% DMSO; Sigma-Aldrich, St. Louis, MO) were implanted subcutaneously on the back of cannulated mice immediately after DTA injection. The minipumps dispensed bretazenil at a rate of 15 ng/h. For immunohistochemistry studies, we perfused mice 4 to 5 h after refeeding.

Immunostaining

We processed mouse brains and cut 10-μm-thick coronal (unless otherwise noted) sections for immunohistochemistry as described (8), using phospho-Akt (pAkt; #4060; Cell Signaling Technology), phospho-Stat3 (pStat3; #9131; Cell Signaling Technology), phospho-ribosomal protein S6 (pS6; #4858; Cell Signaling Technology), and TUNEL kit (Roche Applied Sciences). Sagittal sections and confocal microscopy (LSM710; Zeiss) were used for tracing studies in the hindbrain (scale bar, 100 μm).

RNA Procedures

We extracted RNA with TRIzol (Invitrogen) and reverse transcribed with SuperScript II reverse transcriptase. We performed quantitative PCR using primers spanning introns. Primer sequences are available upon request.

Flow Cytometry and Quantification of Neurons

We dissociated mediobasal hypothalami from neonates with the papain dissociation kit (Worthington Biochemical). We gated live neurons to collect Rfp-positive and/or Gfp-positive neurons. We analyzed the FACS data using FlowJo software. We quantified Glut4, neuropeptide Y (NPY), and proopiomelanocortin (POMC) neurons in adults by counting fluorescent cells in arcuate nucleus (ARH) sections using ImageJ software.

Statistical Analyses

We analyzed data with Student *t* test or one-way ANOVA using GraphPad Prism and Partek Genomic Suite software. We used the customary threshold of $P < 0.05$ to declare statistical significance.

RESULTS

Ablation of Basal Hypothalamic Glut4 Neurons in Adult Mice

Mice are not susceptible to DTA, due to lack of diphtheria toxin receptor (DTR) (10). We took advantage of this property and introduced a *Rosa-iDTR* transgene expressing DTR into *Glut4-Cre* mice to generate *Glut4-Cre*; *Rosa-iDTR* mice. DTR is inserted into the *Rosa26* locus and maintained inactive by a *lox-stop-lox* sequence preceding the DTR cDNA. Upon Cre-mediated excision, the *lox-stop-lox* sequence is removed, leading to DTR expression, and rendering Glut4-expressing cells susceptible to DTA in *Glut4-Cre*; *Rosa-iDTR* mice.

To ablate basal hypothalamic Glut4 neurons, we delivered DTA to that location by stereotactic injection. Forty-eight hours after DTA injection, we killed mice and performed terminal deoxynucleotidyl TUNEL to document cell loss. We detected TUNEL-positive cells in the basal hypothalamus, including arcuate, ventromedial, and lateral hypothalamic nuclei, with sporadic distribution to the dorsomedial nucleus (Fig. 1*A*). We did not see any TUNEL-positive cells in other brain regions, including regions with high levels of Glut4 expression, such as hippocampal field CA1 and dentate gyrus (Fig. 1*A*) (4). In addition, we did not detect peripheral toxicity induced by DTA in Glut4-expressing tissues outside the CNS,

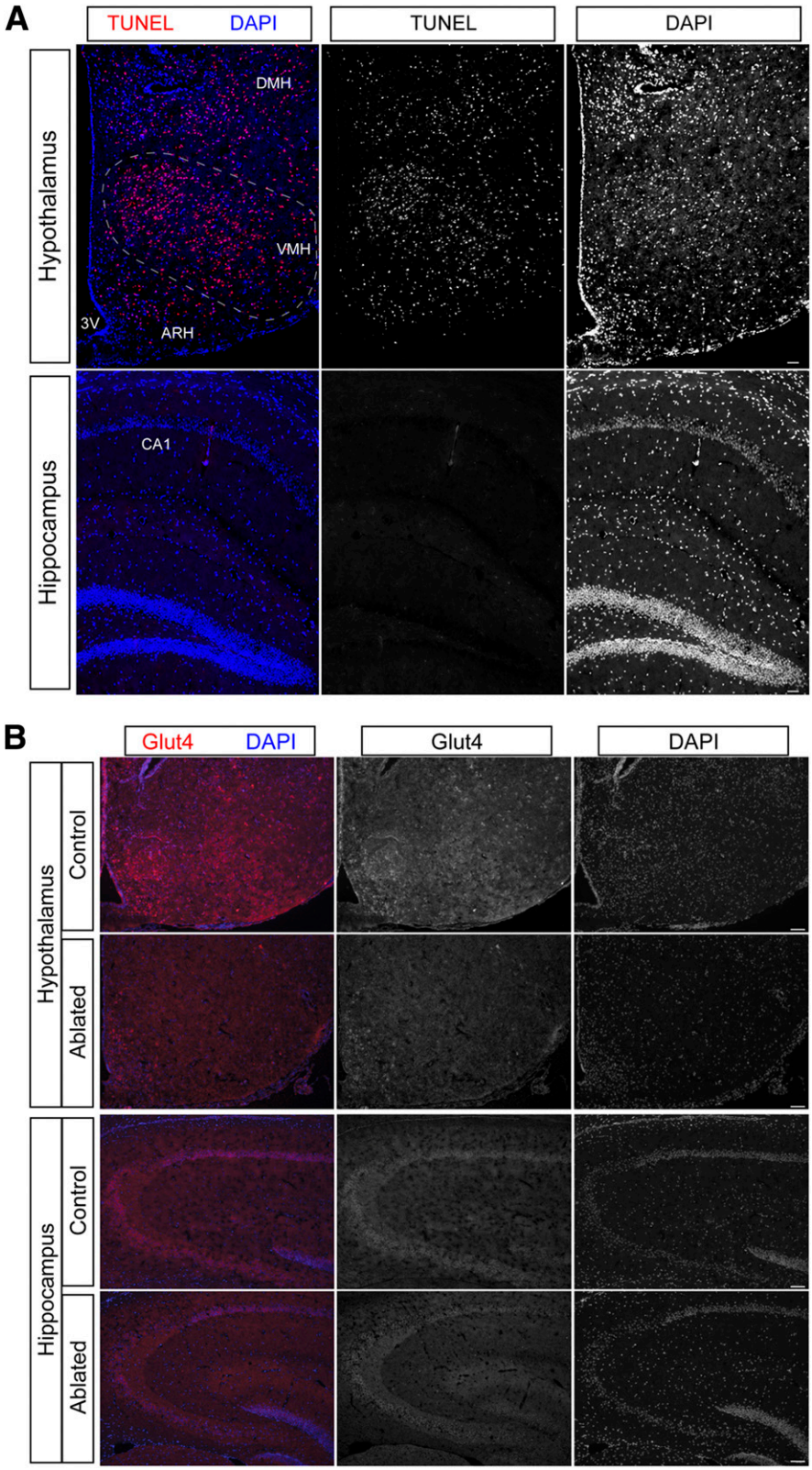

Figure 1—Basal hypothalamic Glut4 neuron ablation. *A*: Basal hypothalamic Glut4 neuron ablation. TUNEL staining of hypothalamus and hippocampus obtained 48 h after DTA injection. Left panel: Merged TUNEL and DAPI staining; middle panel: TUNEL staining; and right panel: DAPI staining. *B*: Representative images of Glut4 immunohistochemistry in control and Glut4 neuron–ablated mice 2 months after DTA injection.

such as muscle and fat (data not shown). To confirm the loss of Glut4 neurons, we performed immunostaining with Glut4 antibody (Fig. 1*B*). Glut4 neurons were detectable in the basal hypothalamus of control mice, but were absent in the ablated mice (Fig. 1*B*). As a control, hippocampal Glut4 neurons were well preserved (Fig. 1*B*).

Changes in Energy Homeostasis After Glut4 Neuron Ablation

Three days after DTA injection, we began to see changes in energy homeostasis concomitant with the onset of neuronal apoptosis. Glut4 neuron–ablated mice showed significant reductions of oxygen consumption VO_2 (Fig. 2*A*) and respiratory quotient (RQ) during the dark phase of the light cycle (Fig. 2*C*), indicating impaired energy use. In contrast, locomotion remained normal throughout the light cycle (Fig. 2*E*). Food intake was severely curtailed during the dark phase (Fig. 2*G*). The pronounced anorexia after Glut4 neuron ablation is expected to yield a negative energy balance.

It could be argued that any extensive ablation of basal hypothalamic neurons would impair eating as a result of tissue reaction, inflammation, and associated vascular changes. Therefore, as a control, we performed neuronal ablations in mice carrying a Cre-inducible DTR in POMC neurons (*Pomc-Cre*; *Rosa-iDTR*), a known effector population of anorexigenic signals. As expected, POMC neuron ablation caused opposite effects to Glut4 neuron ablation. POMC neuron–ablated mice exhibited normal VO_2 (Fig. 2*B*), increased RQ (Fig. 2*D*), reduced locomotor activity during the dark phase (Fig. 2*F*), but increased food intake throughout the light cycle (Fig. 2*H*). The change in food intake is consistent with previous POMC ablation experiments (11), as well as with impaired melanocortin signaling (12).

Compared with POMC neurons, Glut4 neurons constitute a much larger population, and their ablation may cause significant inflammation. To examine the contribution of the inflammatory response to the observed phenotype, we measured hypothalamic expression of mRNA encoding the astrocyte marker, *Gfap*, as a marker of gliosis. *Gfap* was significantly elevated after Glut4 neuron ablation (Supplementary Fig. 1*A*). Next, we measured other markers of inflammation, including interleukins (ILs) and Toll-like receptors (Tlrs). Levels of IL-1, IL-6, IL-12, and tumor necrosis factor-α showed a trend toward increase in samples from Glut4 neuron–ablated mice, but were exceedingly low (i.e., threshold cycle values between 33 and 39), raising the question of whether they are pathophysiologically significant (Supplementary Fig. 1*B*–*E*). In contrast, Tlr2 and Tlr4, for which threshold cycle values were in the usual range (~25), were either unaltered or significantly reduced (Supplementary Fig. 1*F* and *G*). Therefore, the inflammatory response is mainly associated with gliosis.

To rule out that the observed changes of food intake were due to the acute gliosis, we followed mice for up to 2 months after ablation and characterized the metabolic consequences of removing Glut4 neurons. The anorectic effect of Glut4 neuron ablation leveled off, but persisted. Throughout the light cycle, Glut4 neuron–ablated mice continued to show significantly lower cumulative food intake (Fig. 3*A*). Quantitative analyses of the data showed a 23% reduction of food intake during the dark phase (Fig. 3*B*). Interestingly, Glut4 neuron–ablated mice showed increased O_2 consumption (Fig. 3*C* and *D*) and energy expenditure (Fig. 3*I* and *J*), which were not observed immediately after ablation. RQ (Fig. 3*E* and *F*) and locomotor activity (Fig. 3*G* and *H*) were comparable with control mice. Overall, the negative energy balance phenotype persisted throughout the duration of the study. Therefore, we conclude that Glut4 neurons promote positive energy homeostasis by regulating food intake and energy expenditure.

Feeding Behavior After Glut4 or POMC Neuron Ablation

We further characterized the response to fasting and refeeding in Glut4 neuron– or POMC neuron–ablated mice. Glut4 neuron–ablated mice had 50% lower locomotion during fast, indicating reduced foraging (Fig. 4*A*). They showed lower rebound food intake (Fig. 4*B*). To test whether Glut4 neuron–ablated mice had defective responses to orexigenic neuropeptides, we administered intracerebroventricular NPY before and after Glut4 neuron ablation and found identical responses (Fig. 4*C*), indicating that animals can still respond to orexigenic cues. In contrast to the anorexigenic effect observed in Glut4 neuron–ablated mice, mice with POMC neuron ablation displayed hyperphagia (Fig. 4*D*), and increased body weight (Fig. 4*E*).

Glut4 neuron ablation causes persistent negative energy balance, while POMC neuron ablation causes positive energy balance. As a result, 2 months after neuronal ablation, Glut4 neuron–ablated mice showed a 26% decrease in body weight (Fig. 4*F*), while POMC neuron–ablated mice showed a 60% increase (Fig. 4*H*). The changes in body weight reflected changes in adiposity, as Glut4 neuron–ablated mice showed a 3.6-fold decrease of epididymal fat weight (Fig. 4*G*), while POMC neuron–ablated mice showed a 3.5-fold increase (Fig. 4*I*). Moreover, we assayed energy balance in a diet-induced obesity model, in which mice were fed HFD to induce weight gain. NCD-fed mice were injected with DTA and switched to HFD on day 0 (Fig. 4*J*). Although feeding on a more calorie dense diet blunted the weight loss in Glut4 neuron–ablated mice (Fig. 4*J*, ablated HFD vs. ablated NCD), these mice still failed to gain weight compared with controls on HFD (Fig. 4*J*, control HFD vs. ablated HFD). Therefore, we conclude that Glut4 neurons are orexigenic neurons that promote feeding.

CNS Mechanisms of the Anorexigenic Effects of Glut4 Neuron Ablation

We considered different possibilities to explain the remarkable anorexia associated with Glut4 neuron ablation. First, we evaluated ARH neuropeptides. We assessed the

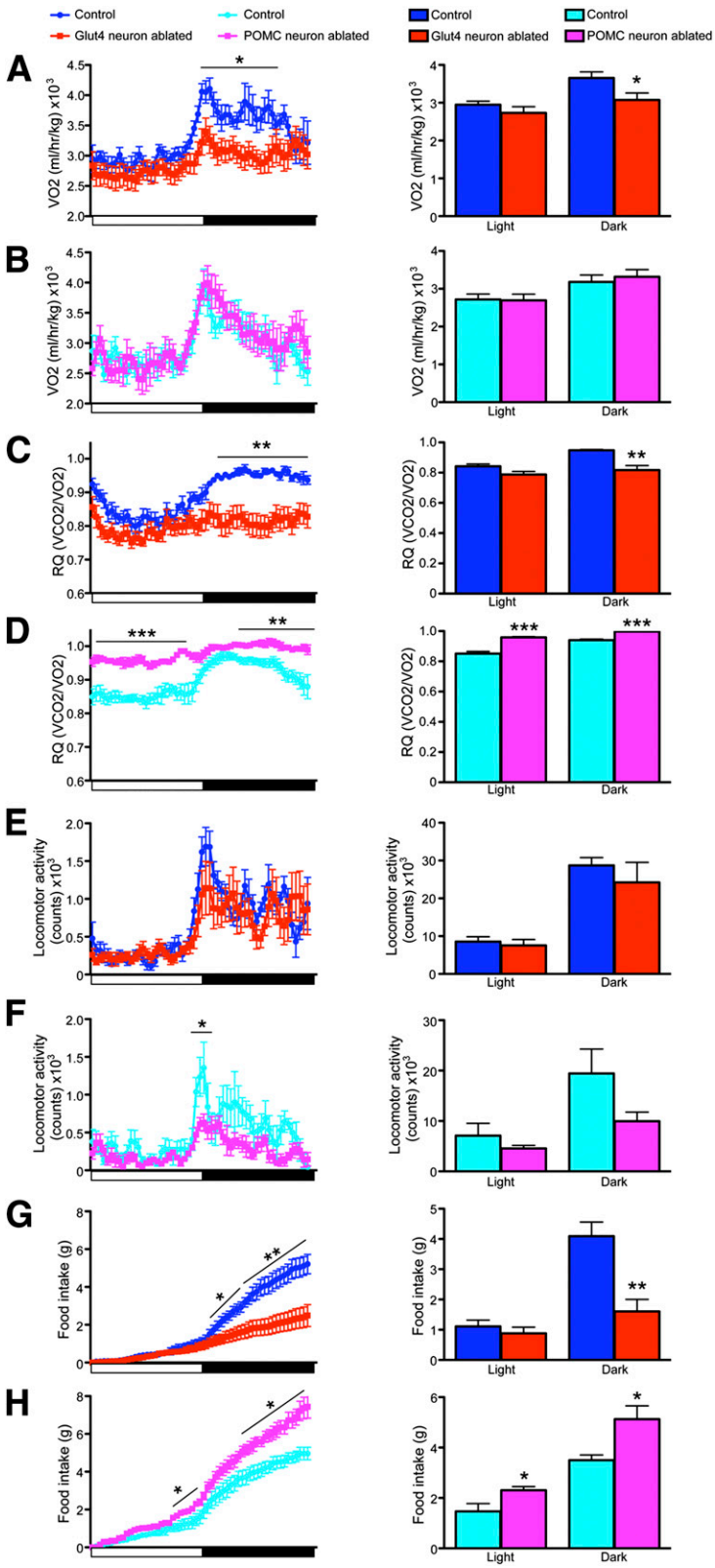

Figure 2—Energy balance 3 days following Glut4 neuron or POMC neuron ablation. Representative continuous 24-h recordings (left) and quantification (right) of VO_2 during the light and dark phases of the light cycle in Glut4 neuron–ablated (*A*) or POMC neuron–ablated (*B*) vs. control mice. Representative continuous 24-h recordings of RQ (left) and quantification (right) in Glut4 neuron–ablated (*C*) or POMC neuron–ablated mice (*D*) vs. controls. Representative continuous 24-h recordings of locomotor activity (left) and quantification (right) in Glut4 neuron–ablated (*E*) or POMC neuron–ablated mice (*F*) vs. controls. Representative continued 24-h recordings of food intake (left) and quantification (right) in Glut4 neuron–ablated (*G*) or POMC neuron-ablated mice (*H*) vs. controls. Data show means ± SEM (n = 8) (*P < 0.05; **P < 0.01; ***P < 0.001).

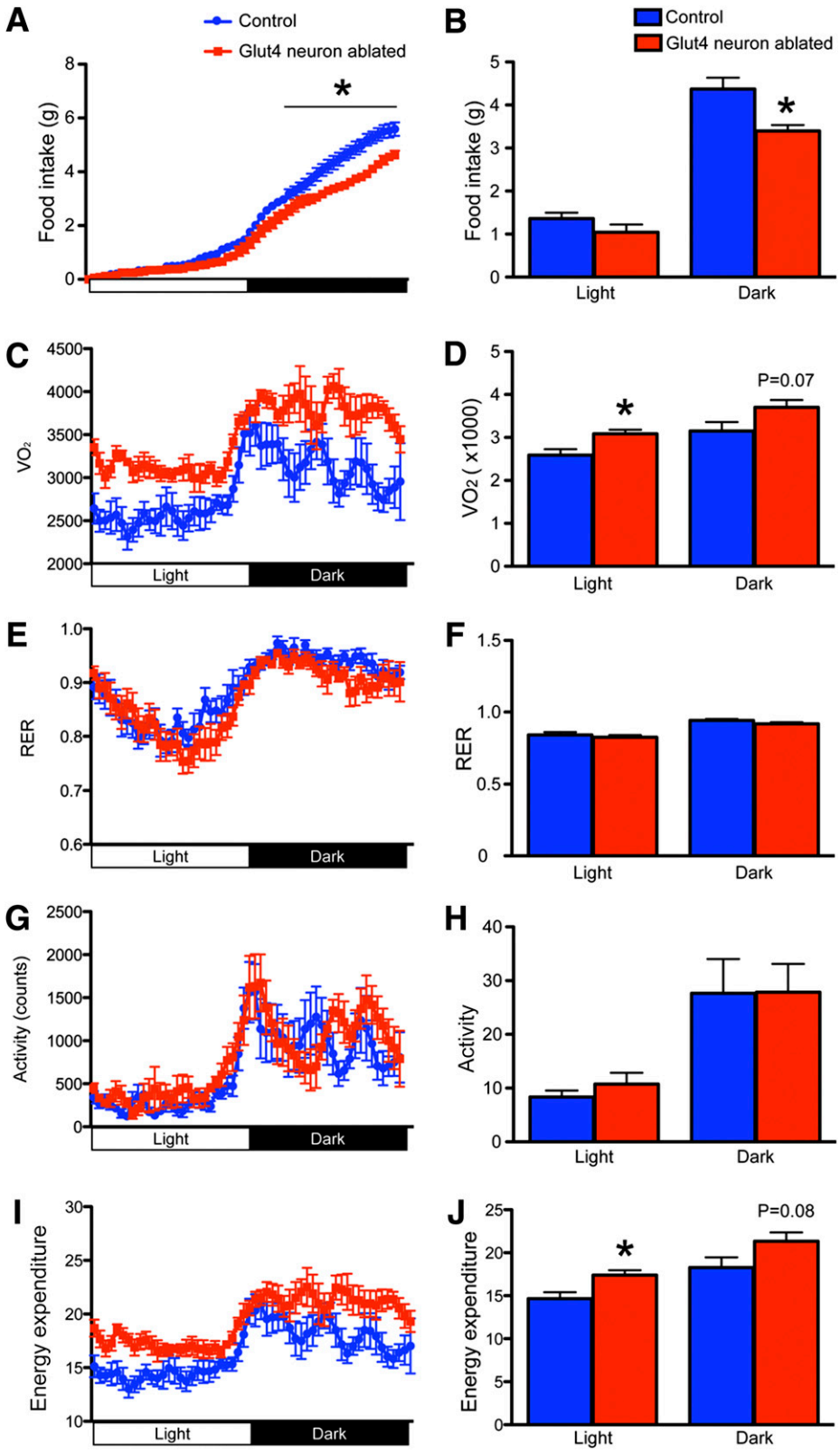

Figure 3—Energy balance 2 months following Glut4 neuron ablation. Twenty-four–hour recording (*A*) and quantification (*B*) of food intake. Twenty-four–hour recording (*C*) and quantification (*D*) of VO_2. Twenty-four–hour recording (*E*) and quantification (*F*) of respiratory exchange ratios (RER). Twenty-four–hour recording (*G*) and quantification (*H*) of total locomotor activity. Twenty-four–hour recordings (*I*) and quantification (*J*) of total energy expenditure. Data show means ± SEM (n = 6–8/group) (*$P < 0.05$).

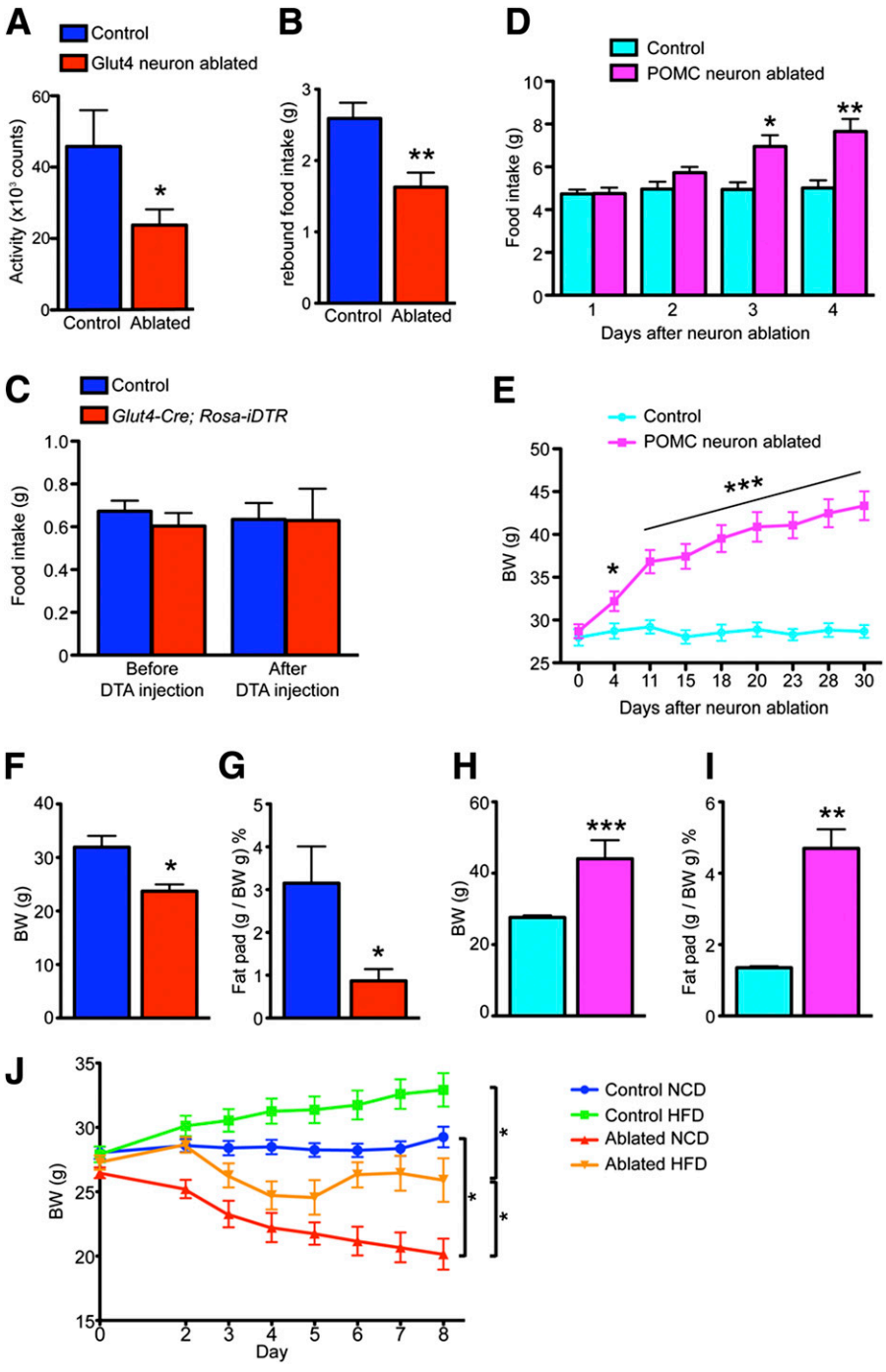

Figure 4—Feeding behavior after Glut4 or POMC neuron ablation. *A*: Locomotor activity during an overnight fast. *B*: Rebound food intake after an overnight fast. *C*: Feeding response to intracerebroventricular NPY injection. *D*: Daily food intake during the first 4 days following POMC neuron ablation. *E*: Time course of body weight (BW) gain in mice with POMC neuron ablation and controls. Comparison of BW (*F* and *H*) and epididymal fat pad weight (*G* and *I*) in mice with Glut4 neuron ablation versus with POMC neuron ablation at the end of the experiment (2 months). *J*: BW measurement after Glut4 neuron ablation on NCD or HFD. Data show means ± SEM ($n = 8$) (*$P < 0.05$; **$P < 0.01$; ***$P < 0.001$).

extent to which Glut4 neurons overlap with agouti-related protein (AgRP)/NPY or POMC neurons. We generated *Glut4-Cre*; *Rosa26-tomato*; *Npy-Gfp* mice and *Glut4-Cre*; *Rosa26-tomato*; *Pomc-Gfp* mice (Supplementary Fig. 2*A*). In both strains, Glut4 neurons are labeled red, whereas NPY or POMC neurons are labeled green. Quantitative analyses showed limited overlap of Glut4 neurons with either NPY (~17%) or POMC neurons (~13%) (Supplementary Fig. 2*B*). We also quantified the percentage of NPY- or POMC-positive hypothalamic Glut4 neurons by flow cytometry (Supplementary Fig. 2*C–F*, upper right quadrants). In the absence of *Glut4-Cre*, we detected no

Tomato signal in NPY (Supplementary Figure 2*C*) or POMC neurons (Supplementary Fig. 2*E*). When Tomato expression was activated by *Glut4-Cre*, ~18% of NPY neurons (Supplementary Figure 2*D*) and ~23% of POMC neurons in the mediobasal hypothalamus (Supplementary Fig. 2*F*) were Glut4 positive.

We measured *Npy/Agrp* and *Pomc* mRNA in Glut4 neuron–ablated mice, but found only a nonsignificant trend toward increased *Agrp/Npy* (Supplementary Fig. 2*G*), consistent with the limited colocalization. Therefore, the anorexigenic phenotype observed in Glut4 neuron–ablated mice was not due to defects in NPY/AgRP and POMC neurons. Curiously, this neuropeptide expression pattern mirrors that seen after ablating orexigenic Rip_{HER} neurons (13), thereby providing further evidence that Glut4 neurons are orexigenic in nature.

Next, we examined other hypothalamic regions that control food intake and energy balance. The lateral hypothalamus (LH) regulates food intake and glucose metabolism (14). Melanin-concentrating hormone (MCH) is a potent orexigen that is produced from Pmch synthesized by LH neurons and acts through Mchr1/r2 receptors (15). Following toxin-mediated ablation of MCH neurons, mice become hypophagic, lean (16), and hyperactive (17). Using MCH immunohistochemistry in *Glut4-Cre*; *Rosa-Gfp* mice, we found that Glut4 and MCH colocalize in the LH (Fig. 5*A*). Moreover, immunohistochemistry demonstrated a sizable decrease in number and intensity of Glut4 staining following toxin-mediated ablation (Fig. 5*B*), indicating potential defects in the MCH system. In fact, *Pmch* expression was significantly reduced in hypothalamic samples after ablation (Fig. 5*C*). Thus, hypothalamic Glut4 neuron ablation affects MCH neuron number and decreases *Pmch* levels, providing a potential explanation for the hypophagia.

Recent work has implicated GABAergic transmission in orexigenic signaling (18). Transcriptome analyses showed that GABAergic signaling elements are enriched in Glut4 neurons (19). Following Glut4 neuron ablation, key genes required for GABAergic signaling, such as *glutamate decarboxylase 1* (*Gad1*), *GABA-A receptor γ1* (*Gabrg1*), and *GABA vesicular transporter member 1* (*vGat*) were decreased (Fig. 5*D*), consistent with the possibility that GABAergic activity is reduced. To test the hypothesis that decreased GABAergic signaling underlies hypophagia, we infused the GABA receptor agonist bretazenil into the mediobasal hypothalamus after Glut4 neuron ablation. Before ablation, all treatment groups showed comparable food intake (data not shown). After ablation, the control group, regardless of whether they received saline or bretazenil, ate comparably to preablation. As expected, Glut4 neuron–ablated mice treated with saline had significantly reduced food intake (Fig. 5*E*). In contrast, the Glut4 neuron–ablated group that received bretazenil partly recovered food intake, even though it was not normalized to preablation levels. Saline or bretazenil infusion was continued for 14 days. Bretazenil infusion attenuated the weight loss caused by Glut4 neuron ablation (Fig. 5*F*).

Altered Glucose Homeostasis After Glut4 Neuron Ablation

Insulin signaling in the CNS affects systemic insulin sensitivity and glucose metabolism (20). We tested whether ablating Glut4 neurons alters peripheral metabolism. Glut4 neuron–ablated mice had significantly elevated fasting glucose and normal ad libitum glucose (Fig. 6*A*, Supplementary Fig. 3*A* and *C*). This is in contrast with elevated ad libitum and fasting glucose in POMC neuron–ablated mice (Supplementary Fig. 3*B* and *D*). Glut4 neuron–ablated mice had comparable glucagon levels (Fig. 6*B*), but significantly reduced insulin during fasting and refeeding (Fig. 6*C*). These findings suggest that the hyperglycemia results from insufficient insulin levels. Immunohistochemical and morphometric studies indicated that β- and α-cell distribution and mass were normal in Glut4 neuron–ablated mice (Supplementary Fig. 3*E*), suggesting that the reduced plasma insulin is likely to reflect insufficient insulin secretion rather than decreased cell number.

Ablating Glut4 neurons impaired glucose tolerance (Fig. 6*D* and *E*) and increased plasma glucose levels during pyruvate tolerance tests (Fig. 6*F* and *G*). As the complexity of the manipulations required for neuronal ablation prevented us from subjecting mice to clamps, we examined liver gene expression for surrogate markers of hepatic insulin resistance. After an overnight fast, *glucose-6-phosphatase* (*G6pc*) and *phosphoenolpyruvate carboxykinase 1* (*Pck1*) increased by 2.4- and 1.8-fold, respectively (Fig. 6*H*). After refeeding, Glut4 neuron–ablated mice showed a 4.3-fold increase of hepatic *G6pc* (Fig. 6*I*), but comparable *Pck1* expression (data not shown). *Pyruvate dehydrogenase kinase 4* (*Pdk4*) controls the activity of pyruvate dehydrogenase in an insulin-inhibitable manner, limiting conversion of pyruvate to acetyl-CoA. Glut4 neuron–ablated mice had significantly increased hepatic *Pdk4* expression after refeeding, consistent with reduced plasma insulin levels (Fig. 6*I*). Curiously, expression of *sterol regulatory element-binding protein* (*Srebp1c*) was nearly fourfold higher under refed, but not fasted conditions (Fig. 6*H* and *I*) and was associated with increased hepatic triglyceride content in Glut4 neuron–ablated mice (Fig. 6*J*). The increased hepatic lipid content in Glut4 neuron–ablated mice may be caused by increased de novo lipogenesis through sterol regulatory element-binding protein and/or increased lipolysis from adipose tissue, due to lower insulin levels.

Glut4 Neurons Project to the Paraventricular Nucleus and Vagal Dorsal Motor Nucleus

To understand the mechanism of defective pancreatic endocrine function in Glut4-ablated mice, we sought to determine their efferent pathways using neuron-tracing studies. We injected adenoviral Ad-iZ-EGfpf in the basal hypothalamus of Glut4-Cre mice. This virus allows for Cre-dependent expression of membrane-tethered, farnesylated Gfp (21). We traced Gfp-labeled projections to two main sites, the vagal dorsal motor nucleus in the

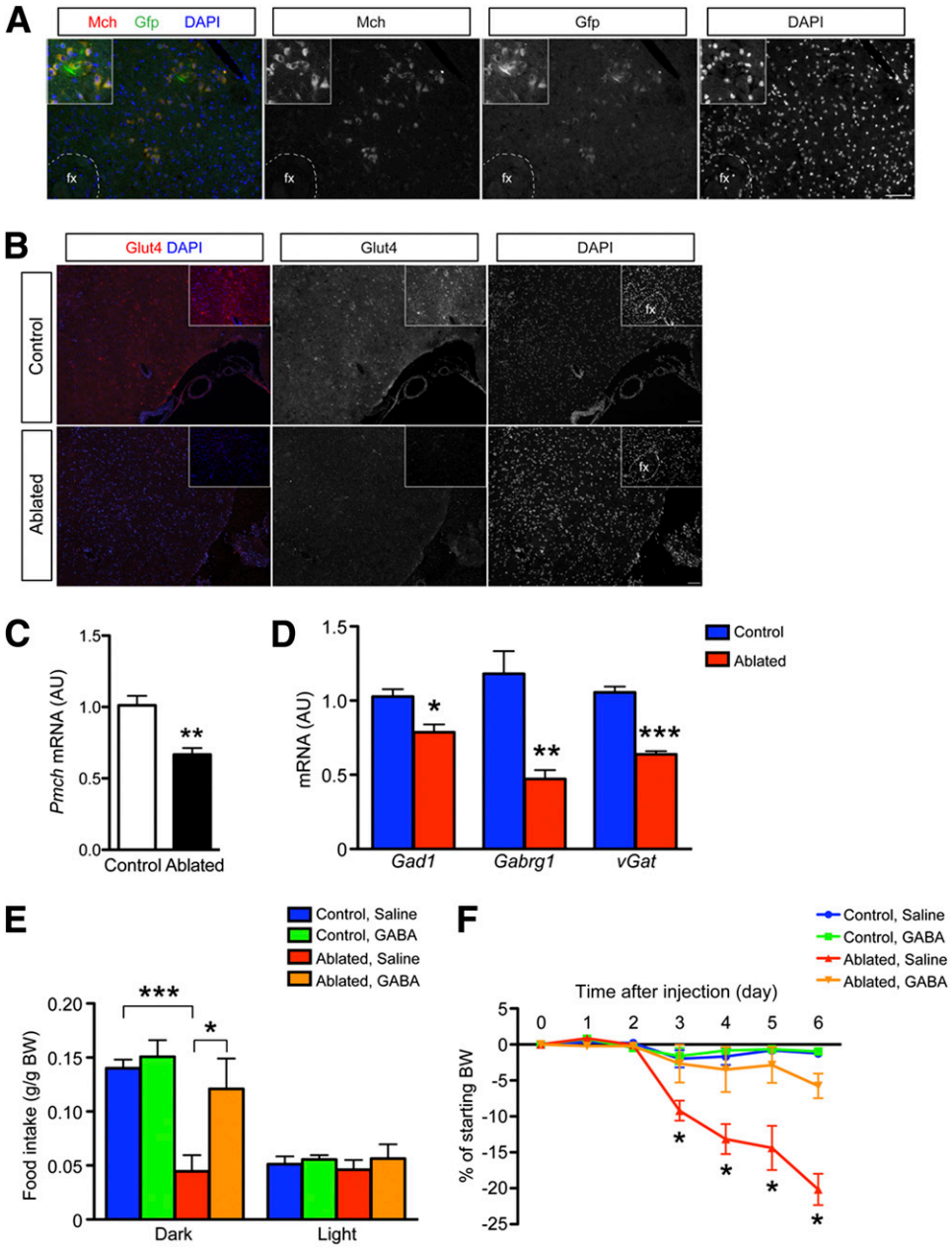

Figure 5—Reduced MCH and GABAergic pathways after Glut4 neuron ablation. *A*: Immunohistochemistry of MCH and Glut4-Cre-Gfp neuron reporter in the LH. *B*: Glut4 immunohistochemistry in the LH after DTA-mediated ablation. *C*: Reduced *Pmch* expression after Glut4 neuron ablation. Data show means ± SEM (n = 6). *D*: Expression of selected components of GABAergic signaling pathways in Glut4 neuron–ablated and control mice (n = 8). *E*: Food intake during the dark and light phases of the light cycle in control and Glut4 neuron–ablated mice infused with saline or GABA agonist. *F*: Time-course analysis of mice receiving GABA or saline infusion after Glut4 neuron ablation (n = 4–6). Data show means ± SEM (*P < 0.05; **P < 0.01; ***P < 0.001). AU, arbitrary unit; BW, body weight; fx, fornix.

hindbrain and the hypothalamic paraventricular nucleus (PVN) (Fig. 7*A*). Vagal dorsal motor nucleus is critical for the regulation of pancreatic secretion, as well as sympathetic and parasympathetic afferents (22,23). Thus, Glut4 neuron ablation causes reduced insulin secretion via impaired vagal efferent to the pancreas. Moreover, we examined c-fos expression as readout of neuronal activation after Glut4 neuron ablation. The c-fos immunoreactivity localized to the PVN, dorsomedial hypothalamus (DMH), and, most prominently, anterior paraventricular thalamic nucleus (Fig. 7*B*). PVN and DMH relay feeding and metabolic cues from the ARH (13,24,25). The findings are consistent with the possibility that Glut4 neurons are integrated with critical hypothalamic nuclei that regulate food intake and hindbrain nuclei that regulate insulin secretion.

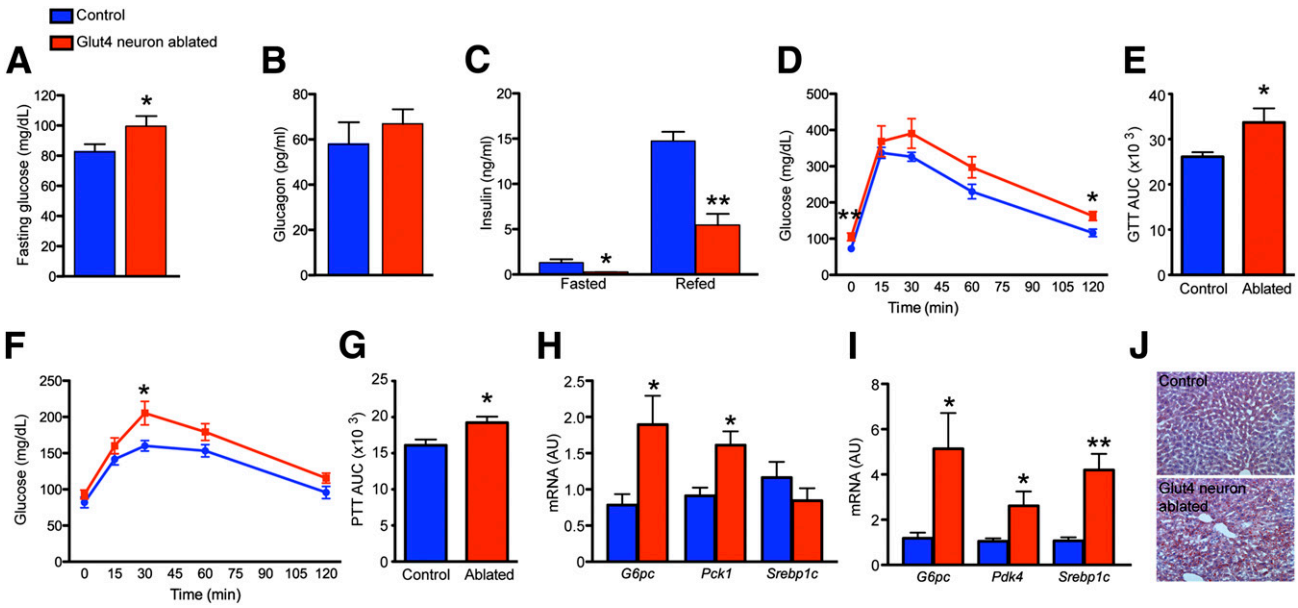

Figure 6—Glucose metabolism in mice 2 months after Glut4 neuron ablation. *A*: Blood glucose after overnight fast. *B*: Plasma glucagon. *C*: Fasting and refed plasma insulin levels. *D* and *E*: Intraperitoneal glucose tolerance tests (GTT). *F* and *G*: Intraperitoneal pyruvate tolerance tests (PTT). *H* and *I*: Hepatic gluconeogenic and lipogenic gene expression during fasting and refeeding. *J*: Hepatic lipid content in fed control and Glut4 neuron–ablated mice. Data show means ± SEM (n = 8) (*P < 0.05; **P < 0.01). AU, arbitrary unit; AUC, area under the curve.

Impaired Hypothalamic Insulin Signaling After Glut4 Neuron Ablation

The changes in energy homeostasis and peripheral metabolism following Glut4 neuron ablation suggest that Glut4 neurons mediate CNS actions of metabolic hormones. To test this hypothesis, we explored hormone signaling following Glut4 neuron ablation. First, we measured pAkt after acute ablation to correlate metabolic phenotypes (Fig. 2) with insulin pathway. Western blots showed that pAkt increased in the hypothalamus of Glut4 neuron–ablated mice after fasting (Supplementary Fig. 4*A*) and refeeding (Supplementary Fig. 4*B*). The increased pAkt in mice with Glut4 neuron ablation could represent an acute response to inflammation. We did immunohistochemistry to colocalize pAkt and Gfap (Supplementary Fig. 4*C*). We found that increased pAkt could only be partially attributed to glial cells (Gfap-positive cells). The acute increase of pAkt in other cells of Glut4 neuron–ablated mice may be a result of compensation or loss of inhibitory tone from Glut4 neurons.

Next, we measured hypothalamic pAkt 2 months after ablation. We found that pAkt immunoreactivity decreased in the basal hypothalamus of Glut4 neuron–ablated mice compared with WT (Fig. 8*A*, left panel), indicating impaired insulin signaling. Leptin signaling, assessed from the number of pStat3-immunoreactive cells (Fig. 8*A* and *B*) as well as their individual intensity (Fig. 8*C*), increased in the basal hypothalamus of Glut4 neuron–ablated mice, despite a significant decrease of fasting and fed plasma leptin (Fig. 8*D*). Glut4 neuron–ablated mice have lower body weight and less adiposity, which can be associated with reduced circulating leptin. However, the change of body weight exceeds the reduction of leptin. Therefore, reduced leptin cannot only be attributed to the reduced body weight, but rather indicates that Glut4 neuron–ablated mice are more leptin sensitive.

We also used pS6 to assess mTOR signaling. We found that generation of pS6 in response to feeding in the hypothalamus of Glut4 neuron–ablated mice was comparable to controls (Fig. 8*A*, right panel). Based on these results, we conclude that disrupting basal hypothalamic Glut4 neurons impairs insulin signaling, but increases leptin signaling and sensitivity.

DISCUSSION

In this study, we sought to define the metabolic functions of basal hypothalamic Glut4 neurons by targeted cell ablation and metabolic phenotyping in adult mice. Combined evidence from these investigations is consistent with a role of this cell population in food intake and glucose metabolism. Key findings of this work are that: *1*) basal hypothalamic Glut4 neurons regulate satiety and glucose homeostasis; *2*) Glut4 neurons regulate energy homeostasis by promoting food intake and reducing energy expenditure; *3*) Glut4 neurons regulate hepatic glucose and lipid metabolism; and *4*) Glut4 neurons regulate insulin secretion and β-cell function, possibly via direct projection to hindbrain. When viewed in the context of previous studies with Glut4-promoter driven insulin receptor knockout (GIRKO) mice (4), the impairment of pAkt immunoreactivity in the current study supports the conclusion that ablating Glut4 neurons causes a defect in

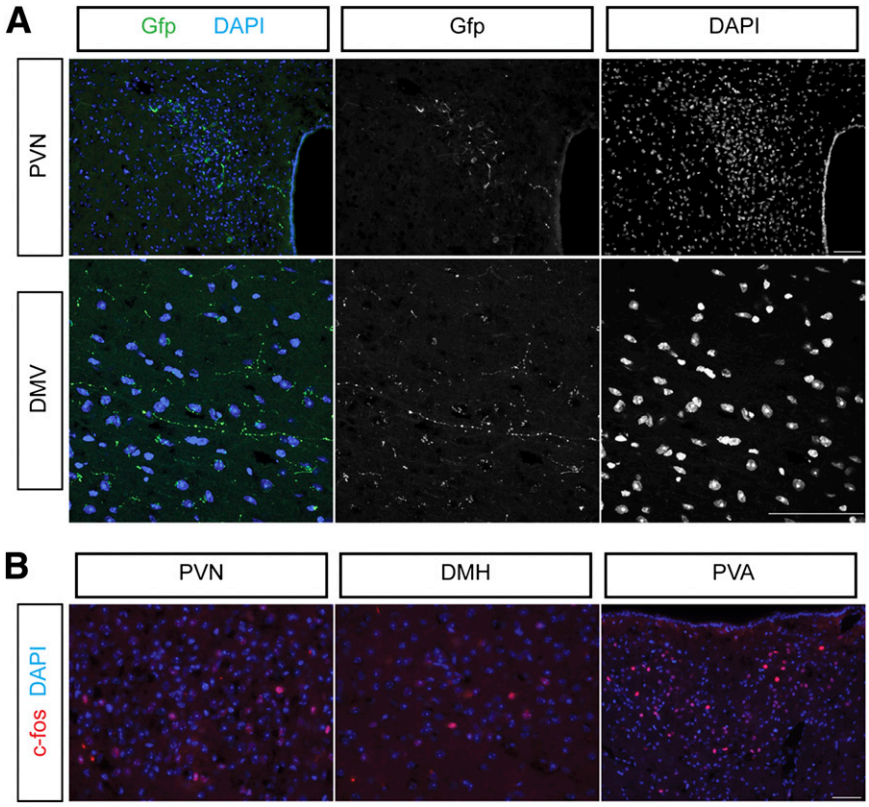

Figure 7—Neural circuit mapping of basal hypothalamic Glut4 neuron projections. *A*: Representative EGfpf fluorescent images following stereotactic injection of iZ-EGfpf to map Glut4 neuron projections. *B*: The c-fos immunohistochemistry 48 h after Glut4 neuron ablation.

the insulin signaling pathway. Qualitative and quantitative changes in pStat3 immunohistochemistry and decreases in plasma leptin levels after ablation indicate that Glut4 neurons normally dampen leptin signaling, emphasizing their integrative role in energy homeostasis. Increased leptin signaling in Glut4 neuron–ablated mice may represent a compensatory response to reduced insulin signaling, consistent with the notion that leptin administration can rescue insulin-deficient diabetes (26). The findings expand our understanding of the neuroanatomy and cellular physiology of insulin action in the CNS and integrate the latter into the broader picture of diabetes pathogenesis.

Glut4 Neuronal Ablation and Inflammation

We detected increased gliosis shortly after Glut4 neuron ablation. Yet, we think that this is unlikely a cause of anorexia. First, the role of inflammation on food intake is complex. Lipopolysaccharide-induced inflammation stimulates the release of cytokines and promotes anorexia (27). In contrast, increased caloric intake associated with an HFD is also associated with hypothalamic inflammation (28). Second, the negative energy balance following Glut4 neuron ablation persisted for 2 months after DTA injection, as did all of the energy balance phenotypes examined in our study. Third, the acute changes in hypothalamic pAkt content are consistent with an anti-inflammatory response. Fourth, Glut4 neuron–ablated mice show reduced weight gain on HFD, which is consistent with negative energy balance.

Glut4 Neurons and Food Intake

The anorectic phenotype linked to Glut4 neuron ablation in the hypothalamus is striking. It bears more than a passing resemblance with that of mice lacking Rip_{HER} neurons, suggesting that the latter partly overlap with the former (13). With regard to the mechanism of this observation, we provide three clues: *1*) Glut4 neurons project to PVN and DMH, two relay sites for feeding cues from the ARH (13,24,25); *2*) Glut4 neurons partly overlap with MCH neurons in the LH, and MCH neuron number and *Pmch* levels fall after Glut4 neuron ablation, potentially contributing to anorexia (29); and *3*) finally, the anorexia can be rescued by GABA supplementation, consistent with an important role of glutamatergic input onto hypothalamic neurons to regulate eating (30–32), as well as with the reversal of starvation caused by NPY neuron ablation (33) by delivery of GABA-A receptor agonists to the hindbrain (18).

Notably, the effects of glutamate and GABA extend to the LH (34). GABA can promote weight gain when released from leptin-inhibited neurons (35). Deleting synaptic release of GABA from Rip_{HER} neurons increases body weight by decreasing energy expenditure and brown

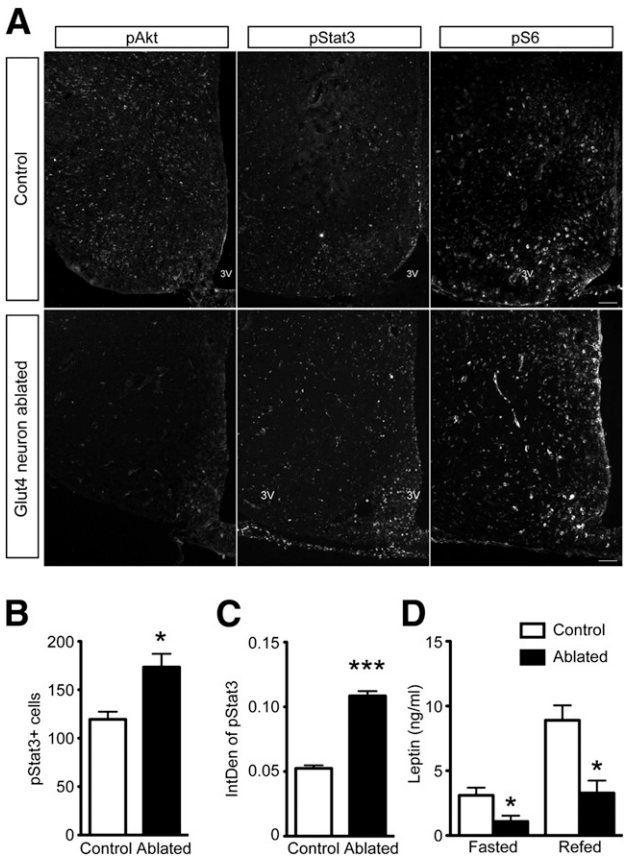

Figure 8—Hormone signaling in the CNS of Glut4 neuron–ablated mice. *A*: Immunohistochemical analysis of pAkt, pStat3, and pS6 in control and Glut4 neuron–ablated mice (2 months after ablation) 4 h after refeeding. Quantification of the number (*B*) and integrative density of individual pStat3-positive cells (IntDen) (*C*) in the ARH (n = 4 to 5 for each group). *D*: Plasma leptin levels in fasted and refed Glut4 neuron–ablated mice (n = 8). Data show means ± SEM (*P < 0.05; ***P < 0.001).

adipose tissue thermogenesis, though not food intake (25). These findings provide more circumstantial evidence that Glut4 neurons feed into these neural circuits.

CNS Regulation of Islet Function and Liver Metabolism

Another key finding of this study is that ablating Glut4 neurons increases hepatic glucose production and decreases insulin levels, suggesting that this neuron population integrates various aspects of metabolic physiology. These observations are consistent with the fact that GIRKO mice (lacking InsR in muscle, fat, and Glut4 neurons) develop diabetes with profound hepatic insulin resistance and β-cell dysfunction (4).

There is a functional link between CNS and pancreatic islet secretion (36). We found that Glut4 neurons are: *1*) enriched in components of the K_{ATP} channel (19), a central regulator of pancreatic hormone release (37); and *2*) project to the vagal DMN, a critical relay station for the CNS–endocrine pancreas axis (38). The alterations of hepatic gene expression and lipid content in Glut4 neuron–ablated mice add to a growing body of evidence linking hypothalamic hormone and nutrient sensing to insulin sensitivity in the liver (39). Whether this process applies to larger mammals remains to be determined (40).

As the medical scientific community scrambles to find new approaches to treat insulin resistance, the fundamental abnormality of type 2 diabetes, the present findings add to a growing catalog of evidence suggesting that the CNS be considered a target organ of insulin sensitizers. In this regard, the identification of a discrete, if heterogeneous, "insulin-sensitive" neuronal population represents a necessary step in developing treatments that meet appropriate standards of safety and efficacy.

Acknowledgments. The authors thank C. Rhodes (University of Chicago) and M.G. Myers (University of Michigan) for providing Ad-iZ-EGfpf adenovirus, X. Xu and A.W. Ferrante (Columbia University) for critical discussion and technical help with assaying inflammation response, and members of the Accili laboratory for critical discussion of the data.

Funding. H.R. is the recipient of a mentor-based postdoctoral fellowship from the American Diabetes Association and the Naomi Berrie Diabetes Research Fellowship. This work is supported by National Institutes of Health grants K99-DK-098294 (to H.R.), 5R37-DK-058282 (to D.A.), and DK-63608 (to Columbia University Diabetes Research Center).

Duality of Interest. No potential conflicts of interest relevant to this article were reported.

Author Contributions. H.R. designed and conducted experiments, analyzed data, and wrote the manuscript. T.Y.L. conducted experiments. T.E.M. provided research tools. D.A. designed experiments, analyzed data, and wrote the manuscript. D.A. is the guarantor of this work and, as such, had full access to all the data in the study and takes responsibility for the integrity of the data and the accuracy of the data analysis.

Prior Presentation. Parts of the study were presented in abstract form at the 71st Scientific Sessions of the American Diabetes Association, San Diego, CA, 24–28 June 2011.

References

1. Kaiyala KJ, Schwartz MW. Toward a more complete (and less controversial) understanding of energy expenditure and its role in obesity pathogenesis. Diabetes 2011;60:17–23

2. Morton GJ, Cummings DE, Baskin DG, Barsh GS, Schwartz MW. Central nervous system control of food intake and body weight. Nature 2006;443:289–295

3. Craft S. The role of metabolic disorders in Alzheimer disease and vascular dementia: two roads converged. Arch Neurol 2009;66:300–305

4. Lin HV, Ren H, Samuel VT, et al. Diabetes in mice with selective impairment of insulin action in Glut4-expressing tissues. Diabetes 2011;60:700–709

5. Accili D. Lilly lecture 2003: the struggle for mastery in insulin action: from triumvirate to republic. Diabetes 2004;53:1633–1642

6. Rayner DV, Thomas ME, Trayhurn P. Glucose transporters (GLUTs 1-4) and their mRNAs in regions of the rat brain: insulin-sensitive transporter expression in the cerebellum. Can J Physiol Pharmacol 1994;72:476–479

7. Leloup C, Arluison M, Kassis N, et al. Discrete brain areas express the insulin-responsive glucose transporter GLUT4. Brain Res Mol Brain Res 1996;38:45–53

8. Plum L, Lin HV, Dutia R, et al. The obesity susceptibility gene Cpe links FoxO1 signaling in hypothalamic pro-opiomelanocortin neurons with regulation of food intake. Nat Med 2009;15:1195–1201

9. Banks AS, Kon N, Knight C, et al. SirT1 gain of function increases energy efficiency and prevents diabetes in mice. Cell Metab 2008;8:333–341

10. Buch T, Heppner FL, Tertilt C, et al. A Cre-inducible diphtheria toxin receptor mediates cell lineage ablation after toxin administration. Nat Methods 2005;2: 419–426
11. Gropp E, Shanabrough M, Borok E, et al. Agouti-related peptide-expressing neurons are mandatory for feeding. Nat Neurosci 2005;8:1289–1291
12. Plum L, Belgardt BF, Brüning JC. Central insulin action in energy and glucose homeostasis. J Clin Invest 2006;116:1761–1766
13. Rother E, Belgardt BF, Tsaousidou E, et al. Acute selective ablation of rat insulin promoter-expressing (RIPHER) neurons defines their orexigenic nature. Proc Natl Acad Sci U S A 2012;109:18132–18137
14. Berthoud HR, Münzberg H. The lateral hypothalamus as integrator of metabolic and environmental needs: from electrical self-stimulation to optogenetics. Physiol Behav 2011;104:29–39
15. Macneil DJ. The role of melanin-concentrating hormone and its receptors in energy homeostasis. Front Endocrinol (Lausanne) 2013;4:49
16. Alon T, Friedman JM. Late-onset leanness in mice with targeted ablation of melanin concentrating hormone neurons. J Neurosci 2006;26:389–397
17. Whiddon BB, Palmiter RD. Ablation of neurons expressing melanin-concentrating hormone (MCH) in adult mice improves glucose tolerance independent of MCH signaling. J Neurosci 2013;33:2009–2016
18. Wu Q, Boyle MP, Palmiter RD. Loss of GABAergic signaling by AgRP neurons to the parabrachial nucleus leads to starvation. Cell 2009;137:1225–1234
19. Ren H, Yan S, Zhang B, Lu TY, Arancio O, Accili D. Glut4 expression defines an insulin-sensitive hypothalamic neuronal population. Mol Metab 2014;3:452–459
20. Koch L, Wunderlich FT, Seibler J, et al. Central insulin action regulates peripheral glucose and fat metabolism in mice. J Clin Invest 2008;118:2132–2147
21. Leinninger GM, Jo YH, Leshan RL, et al. Leptin acts via leptin receptor-expressing lateral hypothalamic neurons to modulate the mesolimbic dopamine system and suppress feeding. Cell Metab 2009;10:89–98
22. Mussa BM, Verberne AJ. The dorsal motor nucleus of the vagus and regulation of pancreatic secretory function. Exp Physiol 2013;98:25–37
23. Laughton WB, Powley TL. Localization of efferent function in the dorsal motor nucleus of the vagus. Am J Physiol 1987;252:R13–R25
24. Atasoy D, Aponte Y, Su HH, Sternson SM. A FLEX switch targets Channelrhodopsin-2 to multiple cell types for imaging and long-range circuit mapping. J Neurosci 2008;28:7025–7030
25. Kong D, Tong Q, Ye C, et al. GABAergic RIP-Cre neurons in the arcuate nucleus selectively regulate energy expenditure. Cell 2012;151:645–657
26. Fujikawa T, Berglund ED, Patel VR, et al. Leptin engages a hypothalamic neurocircuitry to permit survival in the absence of insulin. Cell Metab 2013;18: 431–444
27. Gautron L, Laye S. Neurobiology of inflammation-associated anorexia. Front Neurosci 2009;3:59
28. Thaler JP, Yi CX, Schur EA, et al. Obesity is associated with hypothalamic injury in rodents and humans. J Clin Invest 2012;122:153–162
29. Segal-Lieberman G, Bradley RL, Kokkotou E, et al. Melanin-concentrating hormone is a critical mediator of the leptin-deficient phenotype. Proc Natl Acad Sci U S A 2003;100:10085–10090
30. Pinto S, Roseberry AG, Liu H, et al. Rapid rewiring of arcuate nucleus feeding circuits by leptin. Science 2004;304:110–115
31. Yang Y, Atasoy D, Su HH, Sternson SM. Hunger states switch a flip-flop memory circuit via a synaptic AMPK-dependent positive feedback loop. Cell 2011;146:992–1003
32. Liu T, Kong D, Shah BP, et al. Fasting activation of AgRP neurons requires NMDA receptors and involves spinogenesis and increased excitatory tone. Neuron 2012;73:511–522
33. Luquet S, Perez FA, Hnasko TS, Palmiter RD. NPY/AgRP neurons are essential for feeding in adult mice but can be ablated in neonates. Science 2005; 310:683–685
34. Stanley BG, Willett VL 3rd, Donias HW, Ha LH, Spears LC. The lateral hypothalamus: a primary site mediating excitatory amino acid-elicited eating. Brain Res 1993;630:41–49
35. Xu Y, O'Brien WG 3rd, Lee CC, Myers MG Jr, Tong Q. Role of GABA release from leptin receptor-expressing neurons in body weight regulation. Endocrinology 2012;153:2223–2233
36. Ahrén B. Autonomic regulation of islet hormone secretion—implications for health and disease. Diabetologia 2000;43:393–410
37. Miki T, Liss B, Minami K, et al. ATP-sensitive K+ channels in the hypothalamus are essential for the maintenance of glucose homeostasis. Nat Neurosci 2001;4:507–512
38. Begg DP, Woods SC. Interactions between the central nervous system and pancreatic islet secretions: a historical perspective. Adv Physiol Educ 2013;37:53–60
39. Lin HV, Accili D. Hormonal regulation of hepatic glucose production in health and disease. Cell Metab 2011;14:9–19
40. Ramnanan CJ, Edgerton DS, Cherrington AD. Evidence against a physiologic role for acute changes in CNS insulin action in the rapid regulation of hepatic glucose production. Cell Metab 2012;15:656–664